Iranian Journal of Medical Physics
Vol. 13, No. 4, December 2016, 250-260
Received: September 25, 2016; Accepted: December 07, 2016

Original Article

Monte Carlo Calculation of Shielding Properties of Newly Developed Heavy Concretes for Megavoltage Photon Beam Spectra Used In Radiation Therapy

Rezvan Khaldari[1, 2], Asghar Mesbahi[1,2 *], Umit Kara[3]

Abstract

Introduction

Globally**,** the need for radiotherapy as a part of cancer management increases every year. Thus, the shielding for megavoltage radiotherapy rooms is of great importance.

Materials and Methods

In the present study, 14 types of developed high-density concrete with densities ranging from 2.45 to 5.11$\frac{g}{cm^3}$ were simulated by using Monte Carlo method. The linear attenuation coefficient and the tenth value layer were also calculated. These dosimetric parameters were investigated for megavoltage photon beam spectra for various energies (4, 6, 10, 15, and 18 MeV) of the Varian linac and ^{60}Co gamma rays. The results of simulation were compared with the available published results.

Results

The results showed that the attenuation of high-energy photons is primarily administered by the atomic number and density of the concrete. Moreover, the variation of attenuation coefficient with density was not completely linear.

Conclusion

It was concluded that the attenuation of high-energy photons not only depends on the density of concrete, but also on the atomic number of its composing elements.

Keywords: Monte Carlo Method, High-Density Concrete, Radiation Shielding, Attenuation Coefficient

1- Immunology Research Center, Tabriz University of Medical Sciences, Tabriz, Iran
2- Department of Medical Physics, School of Medicine, Tabriz University of Medical Sciences, Tabriz, Iran
3- Suleyman Demirel University, Vocational School of Health Services, Isparta, Turkey

*Corresponding author: Tel+989141193747; Fax: +98 413 3364660; Email: mesbahiiran@yahoo.com, amesbahi2010@gmail.com

1. Introduction

Radiation shielding concrete (RSC) is one of the most common and versatile materials that used for protection in radiation therapy bunkers. High-density aggregate is utilized in this type of concrete to attenuate and absorb gamma rays in order to prevent radiation leakage from radiotherapy bunkers [1-5].

Many experimental and theoretical studies were conducted on the production of high-density concrete. For example, Ouda studied 15 concrete mixtures, including aggregate of barite, magnetite, goethite and serpentine, for gamma shielding by using ^{137}Cs and ^{60}Co photon sources. It was reported that magnetite, as a fine aggregate, enhances the shielding properties of the concrete against gamma rays [6]. Waly and Bourham also calculated shielding factors theoretically by using computational methodology based on MicroShield program [7]. In another experimental study, Gencel et al. studied the effect of hematite on the gamma and neutron shielding characteristics of heavy concrete [8].

Additionally, new types of heavy concrete based on high atomic number materials such as lead were proposed. For instance, Mortazavi et al. studied the shielding properties of Datolite-Galena concrete using cobalt-60 radiotherapy unit and Am-Be as photon and neutron sources [9]. In this regard, the effects of galena (7.0 – 7.5$\frac{g}{Cm^3}$) with different aggregate such as colematine (2.42$\frac{g}{Cm^3}$) and tourmaline (3.0 - 3.25$\frac{g}{Cm^3}$) were investigated in other studies in order to increase the radiation shielding properties of concrete [10-12]. Abdo calculated shielding factors for gamma rays and fast neutrons by utilizing four types of concrete with different densities, dolomite–sand, barite–barite, magnetite–limonite, and ilmenite–ilmenite [13]. In some other studies, shielding properties of barite-loaded heavy concrete were investigated. The researchers showed that the barite incorporated into concrete can increase the linear attenuation coefficient and protection against radiation [14-26].

In a number of studies, shielding properties of high-density concrete were investigated by using Monte Carlo (MC) method. Calzada et al. studied a new shielding material for neutron and gamma radiation shielding by employing MC code MCNP5 [27]. Singh et al. used MCNP 4B code for calculating mass and linear attenuation coefficients and tenth value layer of seven types of concrete at photon energies of 1.5, 2.0, 3.0, 4.0, 5.0, and 6.0 MeV [28]. Sharifi et al. computed shielding factors of ordinary, barite, serpentine, and steel–magnetite concrete in 511, 662, and 1332 KeV photon energies by using MCNP-4C code [14].

In another experimental study, Aghamiri et al. examined photons and neutron shielding properties of tourmaline-galena as a novel heavy concrete. They applied MCNP4C code for calculating the effects of various shield thicknesses on the attenuation of photons and neutrons [12]. By Using Monte Carlo code of MCNP5, Gencel et al. investigated photon and neutron attenuation characteristics of concrete, including hematite, in different proportions [8]. Finally, Facure and Silva theoretically calculated tenth value layers (TVL) for heavyweight concrete with ferrophosphorus, limonite, ilmenite, magnetite, and barite at high-energy beams by using MCNP5 MC code [29].

In a comprehensive study on shielding properties of heavy concrete, Bashter and Bashter et al. both theoretically and experimentally examined the heavy concrete made of local magnetite ores including hematite-serpentine, ilmenite-limonite, basalt magnetite, ilmenite, steel-scrap, and steel-magnetite at photon energies from 10 KeV to 1 GeV [30, 31].

According to NCRP No. 144 and NCRP No.151, heavy concrete, as a shielding material, has advantages for designing the radiation therapy rooms, especially when space is of concern. Therefore, it is useful for making permanent shields and providing good photon shielding, structural strength, as well as neutron shielding. These advantages enable a heavy concrete to create radiation shielding with lower thicknesses compared to ordinary concrete. One of the few disadvantages of a

heavy concrete is its expensiveness and difficulty in handling [32, 33]. A thorough investigation among the published papers in the literature by the authors of the current paper revealed that most of the developed heavy concretes were evaluated dosimetrically by monoenergetic gamma rays of ^{60}Co and ^{137}Cs sources. Moreover, some of the developed heavy concretes were only investigated by neutron source.

However, it is a laborious process to experimentally determine the radiation attenuation properties of all the newly developed concretes for a wide range of high-energy photons used in radiation therapy. To address this shortage of information and provide more data about the radiation attenuation characteristics of newly proposed heavy concrete, the current MC study was conducted. In order to use heavy concrete in designing radiation therapy facilities, where the main radiation beam can strike the walls and roof, MC method was used to calculate the linear attenuation coefficients for 14 high-density concretes selected from recently published articles at megavoltage photon beam spectra of the Varian LINAC and ^{60}Co [34]. Moreover, the results of MC simulation were compared with the previously published results obtained by Facure and Silva [29]. This study is an attempt to provide new and comparative information on the attenuation coefficient of newly developed heavy concretes in range of megavoltage photon beam spectra used in radiation therapy.

2. Materials and Methods

2.1. Monte Carlo calculations of attenuation coefficient

In the current study, the MCNPX code (2.7.E) was used for our simulations [35]. Photon cross-section data libraries, including mcplib04 and ENDF/B-VI, were applied in the MC simulations. The MCNPX code, developed by Los Alamos National Laboratory, is the internationally recognized code for analyzing neutron- and gamma ray-transport by the MC method. In this study, a good geometry was designed to calculate the attenuation coefficient (μ) of heavy concretes (Figure 1).

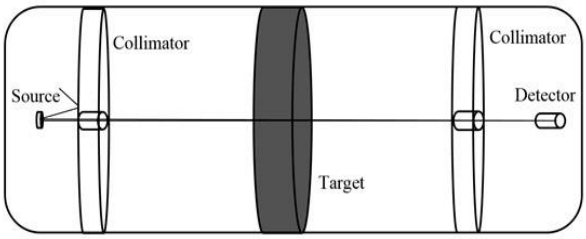

Figure 1. The schematic representation of simulated geometry used for Monte Carlo calculations

The attenuation coefficient (μ) is determined experimentally by using narrow beam geometry, which is sometimes referred to as "good" geometry [36]. Since it does not include field size and scatter effects, photon beams that reach the detector keep all the original energy [37, 38].

A circular plate of 0.5 cm diameter was located 200 cm away from the concrete slab (target) along the –y axis. The photon beam spectra for various energy beams of the Varian linac were used as photon sources. The source was considered as planar with uniform distribution of high-energy photon that emits high energetic photons along +y direction, vertical to the front face of the shields.

In order to minimize the contribution of scatter and secondary radiation, we used very long source-to-target distance and very long target-to-detector distance in this simulation [39]. Collimators were also located in the distance between source-target and target-detector [40]. MC simulation results obtained with less than 2% statistical error [15, 28, 29].

Table 1. The studied concrete and their compositions

Element	Concrete type and density (g cm^{-3})													
	Steel-magnetite 5.11	Ferrophosphorus 4.82	Concrete 6 4.46	Da-Ga[a] 4.42	HDSC 4.0	Steel scrap 4.0	Hormirad 3.99	Ilm–ilm[a] 3.69	Ilmenite 3.5	Barite 3.49	Barite 3.452	Barite 3.35	Hematite 2.768	Peridotite 2.45
H	0.026	0.0210	0.008	0.039	0.021	0.028	0.017	0.023	0.0005	-	0.020	0.012	0.018	0.027
O	0.802	0.3220	1.671	0.770	1.024	0.843	1.247	1.419	1.146	1.007	1.132	1.043	1.001	1.2
Mg	0.029	0.0060	0.011	-	0.004	0.003	0.015	0.006	0.049	0.009	0.015	0.004	0.151	0.587
Al	0.033	0.0090	0.010	0.013	0.017	0.048	0.006	0.013	0.013	0.031	0.013	0.014	0.019	0.003
Si	0.136	0.0090	0.473	0.310	-	0.419	0.074	0.057	0.059	0.043	0.071	0.035	0.102	0.438
P	0.004	1.0490	-	-	-	-	0.011	0.002	-	0.0002	0.0003	-	-	0.0007
S	0.003	0.0040	0.007	0.357	-	0.002	0.0003	0.003	0.0007	0.440	0.360	0.361	0.005	0.001
Ca	0.201	0.2030	0.379	0.509	0.200	0.171	0.173	0.196	0.005	0.024	0.227	0.168	0.658	-
Mn	0.003	0.0130	-	0.006	-	-	0.002	0.005	-	-	0.003	-	0.001	-
Fe	3.869	2.8230	1.339	0.028	2.674	2.45	2.425	1.033	1.395	0.0003	0.010	0.159	0.807	-
Na	-	-	0.001	0.008	-	-	-	0.020	0.002	0.013	0.001	-	0.00005	-
K	-	-	0.003	0.010	-	0.012	0.002	0.009	0.001	-	0.0005	-	0.0001	0.003
C	-	0.0040	0.026	-	-	-	0.001	-	-	0.012	0.012	-	-	-
Pb	-	-	0.675	2.303	-	-	-	-	-	-	-	-	-	-
Ti	-	0.0420	-	-	-	-	0.007	0.900	0.792	-	-	-	0.0002	-
Cl	-	-	-	-	-	-	-	-	0.0007	0.019	0.001	-	-	-
Ba	-	-	-	-	-	-	-	-	-	1.884	1.519	1.552	-	-
Ni	-	0.017	-	-	-	-	-	0.0003	-	-	0.004	-	-	0.0004
Sr	-	-	-	-	-	-	-	-	-	-	0.065	-	-	-
Cr	-	0.0840	-	0.005	-	-	-	-	-	-	-	-	-	-
B	-	-	-	0.046	0.014	-	-	-	-	-	-	-	-	-
V	-	0.0840	-	-	-	-	0.001	-	-	-	-	-	-	-
N	-	-	-	-	-	-	0.0002	-	-	-	-	-	-	-
W	-	-	-	-	-	-	-	-	-	-	-	-	-	0.0008
Co	-	-	-	-	-	-	-	-	-	-	-	-	-	0.0005
Cu	-	0.0080	-	-	-	-	-	-	-	-	-	-	-	-
Mo														

In the first run, the photon source was replaced with 1.25 MeV average beam energy of ^{60}Co. Then, to calculate the attenuation coefficients of the studied concretes in radiation therapy range, the photon beam spectra reported in an article by Sheykh-Bagheri was employed [34]. The applied photon beam spectra for simulation are shown in Figure 2. Fourteen types of developed high-density concretes , with densities ranging from 2.45 to 5.11$\frac{g}{cm^3}$, were studied in this simulation [7-9, 13, 18, 25, 29, 30, 41-45].

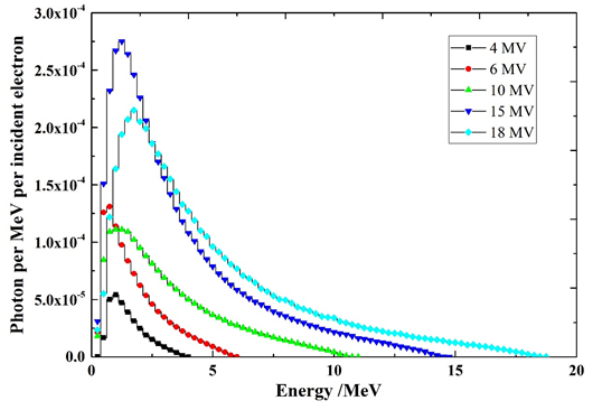

Figure 2. The photon energy spectra used for Monte Carlo calculations derived from Sheykh-Bagheri et al.

Every type of heavy concrete in the form of cylinders was considered and set on y-axis. The thickness of concrete samples ranged from 0 to 30 cm. The composition and density of the studied concretes are shown in Table 1. A small cylinder of 1 cm diameter and 5 cm thickness was set as a detector and recorded the flux averaged over a cell.

The cylinder was located on the other side of the slab and 200 cm away from its surface. The F4 tally was used for scoring primary photons reaching the detector cell. It calculates the photon fluence crossing a detector cell in terms of photon/cm^3 in the MCNPX code. The neutrons and electrons were not scored by the detector cell.

Photon interactions with matter depend on the incoming photon energy [46], which is defined by Lambert's law ($I = I_0\ e^{-\mu t}$) for transmitted intensity through a medium [28]. The most important factor characterizing the penetration and diffusion of X and gamma rays in a medium is linear attenuation coefficient. It is defined as the attenuation of the gamma-ray beam intensity in good geometry per unit thickness of absorber, as described by the following equation:

$$\lim_{\Delta t \to 0} \frac{\Delta I / I}{\Delta t} = -\mu \quad (1)$$

where $\Delta I / I$ is the fraction of the gamma-ray beam attenuated by an absorber of a thickness of Δt [47].

In this work, the simulated geometry was benchmarked with the standard data mentioned in a report by Hubbell in the National Institute of Standards and Technology (NIST) and WinXCom program [48, 49]. For this reason, the attenuation properties of lead (density= 11.35 $\frac{g}{cm^3}$) and the ordinary concrete (density=2.3 $\frac{g}{cm^3}$) [48] were calculated by WinXCom program [49]. The results of our MC model were compared with those of WinXcom for validation of our simulated model.

It should be reminded that WinXcom is the windows version of XCOM that was developed by Berger and Hubbell (1987/99). This program can calculate total cross-sections and attenuation coefficients for simple elements and mixtures [49]. The percentage difference was computed by using this equation:

Percentage error= ((MCNPX − WinXCom)/(WinXCom))×100 (2)

Moreover, DIFF% (1) and DIFF% (2) indicated the percentage difference between MC simulation results and NIST data and between MC simulation results and theoretical data of WinXCom program, respectively.

3. Results

In the present study, the photon shielding properties of various types of some high-density concretes were calculated. In the first step, the validity of our MC model was verified by using WinXCom and NIST data. The results of benchmarking of MC model are shown in Table 2. As it can be noted, the results were in close agreement (less than 1% difference) with

benchmark data and our MC model was validated. In Table 3, linear attenuation coefficients are shown for photon beam spectra of 4, 6, 10, 15, and 18 MeV of Varian linac and for ^{60}Co with 1.25 MeV average energy. Moreover, the relationship between concrete density and linear attenuation coefficient is presented in Figure 3. Figure 4 represents tenth value layer for the studied high-density concrete with different densities for all the studied photon energies. The transmission curves obtained for some of the high-density concrete for the photon beam spectra of 6 and 18 MeV are illustrated in figures 5 and 6, respectively.

Table 2. Benchmarking of Monte Carlo model against the available data on lead and ordinary concrete from WinXcom and NIST

Energy (MeV)	Density ($\frac{g}{cm^3}$)	MCNPX	NIST(1)	WinXCom (2)	DIFF% (1)	DIFF% (2)
0.5	2.3	0.2053	0.2050	0.2050	0.1243	0.1248
	11.35	1.8212	1.8318	1.8312	0.5835	0.5514
1	2.3	0.1496	0.1493	0.1493	0.1439	0.1499
	11.35	0.8025	0.8060	0.8060	0.4437	0.4420
10	2.3	0.0525	0.0523	0.0524	0.2023	0.1870
	11.35	0.5642	0.5643	0.5643	0.0216	0.0216
15	2.3	0.0479	0.04820	0.0481	0.6388	0.6203
	11.35	0.6393	0.6421	0.6421	0.4489	0.4441
20	2.3	0.0467	0.0466	0.0466	0.0214	0.0064
	11.35	0.6981	0.7043	0.7043	0.8917	0.8852

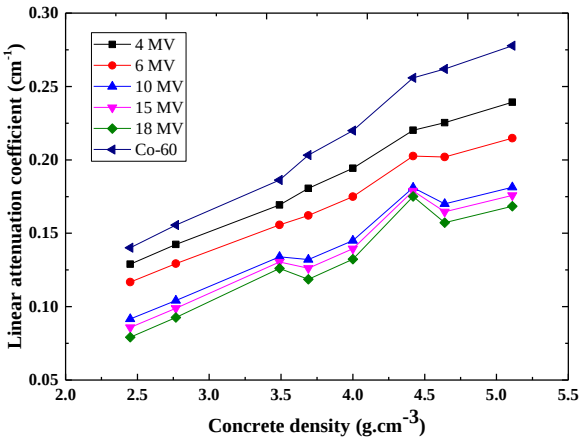

Figure 3. Linear attenuation coefficients (μ,cm^{-1}) of some high-density concrete for photon spectra of 4, 6, 10, 15, and 18 MV and 60Co with 1.25 MV average energy. The ascending arrangement in terms of density for the studied concrete from left to right of the graph is peridotite (2.45 g.cm^{-3}), hematite (2.768 g. cm^{-3}), barite (3.49 g. cm^{-3}), ilmenite-ilmenite (3.69 g. cm^{-3}), steel-scrap (4.0 g. cm^{-3}), datolite-galena (4.42 g. cm^{-3}), concrete 6 (4.64 g. cm^{-3}), ferrophosphorus (4.820 g. cm^{-3}), and steel- magnetite (5.11 g. cm^{-3}).

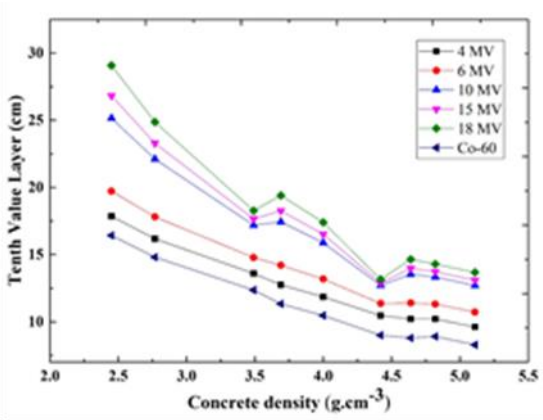

Figure 4. Tenth value layer (TVL) with different high-density concrete at photon energy spectra of 4, 6, 10, 15, and 18 MV and ^{60}Co. The high-density concrete from left to the right are: peridotite (2.45g.cm^{-3}), hematite (2.768g. cm^{-3}), barite (3.49g. cm^{-3}), ilmenite-ilmenite (3.69g. cm^{-3}), steel-scrap (4.0 g. cm^{-3}), datolite-galena (4.42g. cm^{-3}), concrete 6 (4.64g. cm^{-3}), ferrophosphorus (4.820g. cm^{-3}), and steel- magnetite (5.11g. cm^{-3}).

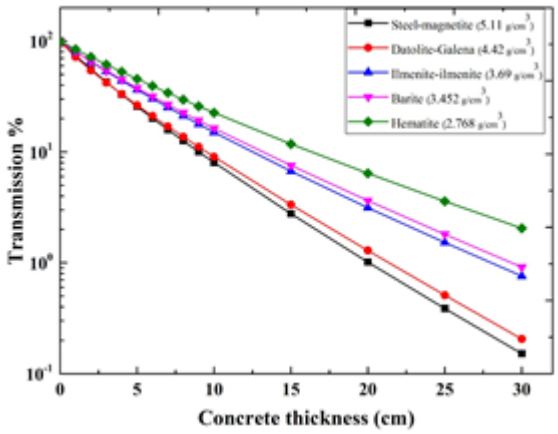

Figure 5. Radiation transmission for thickness of some types of high-density concrete studied at the energy spectrum of 6 MV Varian linac

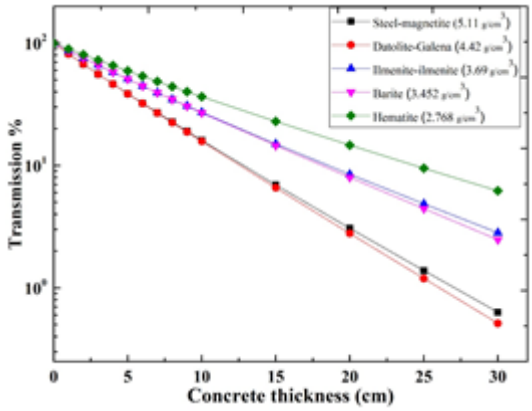

Figure 6. Radiation transmission for thickness of some types of high-density concrete studied at the energy spectrum of 18 MV Varian linac

4. Discussion

In order to obtain reliable results for every MC calculation, it is essential to have minimum differences between MC and benchmark results. Indeed, benchmarking and optimization of our MC model was performed against benchmark data obtained from WinXcom software and NIST. The maximum percentage difference of MC simulation results from WinXCom program and the report by Hubble at NIST for lead and ordinary concrete were obtained at photon energy of 20 MeV with 0.88% and 0.89% error, respectively. Overall, the percentage differences were less than 1% for all the energies and concrete. It is known that linear attenuation coefficient values of materials depend primarily on the incident photon energy, atomic number, and density (ρ) of the shielding materials [50]. Additionally, the value of linear attenuation coefficient decreases as the energy of incident X and gamma rays increases.

Table 3 and Figure 2 graphically present that high-density concretes at high photon energy spectra of 10, 15, and 18 MeV has lower linear attenuation coefficients than the low photon energies of 4, 6 MeV and 1.25 MeV for ^{60}Co. Moreover, the amount of this parameter decreases as the density of the absorber is lowered. As shown in Figure 2, the reduction of linear attenuation coefficients versus concrete density is not linear and there are two peaks at high-energy photon beam. The linear attenuation coefficient at high-energy spectra of 10, 15, and 18 MeV is greater for datolite-galena concrete relative to the others. As the Z of absorber increases, the linear attenuation coefficient becomes greater. The reason is that photoelectric interactions increase in high-Z materials, especially for low-energy photons, and high-Z materials yield more pair production interactions for high-energy photons. Therefore, the high Z atoms used in this concrete, such as Pb and Fe, and more pair production interactions at high- energy photons caused the highest linear attenuation coefficient value among of all the studied concretes.

According to our MC simulation results and the published results of Demir et al., high-density concretes containing barite has high attenuation coefficients, especially at high energy spectra of 10, 15, and 18 MeV. Consequently, it can be concluded that photon radiation shielding property of the concrete, including barite, increases at high photon energies [20].

Table 3. Density of concrete and linear attenuation coefficients at photon beam spectra of 4, 6, 10, 15, and 18 MV and ^{60}Co

Types of concrete and density ($\frac{g}{cm^3}$)	Linear attenuation coefficient (cm^{-1})					
	4 MV	6 MV	10 MV	15 MV	18 MV	^{60}Co
Steel-magnetite (5.11)	0.2393	0.2147	0.1814	0.1758	0.1683	0.2777
Ferrophosphorus (4.820)	0.2253	0.2034	0.1727	0.1677	0.1609	0.2585
Concrete6 (4.64)	0.2253	0.2019	0.1700	0.1646	0.1572	0.2618
Datolite –Galena (4.42)	0.2201	0.2026	0.1811	0.1788	0.1750	0.2558
Steel scrap (4.0)	0.1943	0.1749	0.1449	0.1394	0.1323	0.2199
HDSC (4.0)	0.1935	0.1744	0.1448	0.1394	0.1325	0.2186
Hormirad (3.99)	0.1933	0.1739	0.1436	0.1380	0.1308	0.2188
Ilmenite-ilmenite (3.69)	0.1805	0.1620	0.1320	0.1261	0.1186	0.2032
Ilmenite (3.50)	0.1706	0.1541	0.1262	0.1207	0.1139	0.1902
Barite (3.49)	0.1693	0.1557	0.1339	0.1304	0.1260	0.1862
Barite (3.452)	0.1696	0.1552	0.1319	0.1321	0.1229	0.1872
Barite (3.350)	0.1644	0.1509	0.1286	0.1248	0.1201	0.1806
Hematite(2.768)	0.1423	0.1292	0.1041	0.0988	0.0925	0.1555
Peridotite (2.450)	0.1289	0.1167	0.0915	0.0858	0.0792	0.1401

Moreover, as shown in Figure 2, the non-linear relationship between density and attenuation coefficient at low photon energies of 4, 6 MeV, and ^{60}Co seems to be due to different chemical compositions and various amounts of heavy elements, such as Pb and Fe, in concrete. In pervious published studies, the linear attenuation coefficient was calculated for datolite-galena, ilmenite-ilmenite, barite (3.452 g. cm^{-3}), and hematite concrete at 1.25 MeV. Their reported values of linear attenuation coefficients for these types of concrete at energy of 1.25 MeV were similar (less than 1.5% difference) to our obtained results [8, 9, 13, 44]. However, there was no comparable data for other energies.

According to Figure 4, the value of TVL is in inverse proportion to the concrete density. It was also found that the TVL values increase with the incident photon energy. It can be seen that the minimum value of TVL at high spectrum energies of 10, 15, and 18 MeV belongs to datolite-galena concrete with density of 4.42 $\frac{g}{cm^3}$. Moreover, steel-magnetite concrete with density of 5.11$\frac{g}{cm^3}$ has the lowest TVL value for photon energy spectra of 4, 6 MeV and 1.25 MeV of ^{60}Co.

Facure and Silva calculated TVL for some high-density concretes, including ferrophosphorus, with the photon spectra measured by Mohan et al. [29]. Our results for ferrophosphorus concrete can be compared with their results at the photon energy spectra of 4, 6, and 10 MeV. For these energies, our computed TVLs for this concrete were lower (about 15%) than those calculated by Facure and Silva. This discrepancy can be explained by the variation in photon energy spectra used in both studies. In the current study, MC

calculations were performed using the updated photon beam spectra proposed by Sheykh-Bagheri and Rogers [34].

As can be observed in Figure 5, at the energy spectrum of 6 MeV, steel–magnetite concrete with the highest density shows higher radiation attenuation and has the lowest transmission among the studied concretes. It means that density has a greater impact, as compared to effective atomic number of a concrete for the 6 MeV spectrum. However, when the energy spectrum becomes 18 MeV (Figure 6), although steel-magnetite concrete has higher density than datolite-galena concrete, datolite-galena represents higher attenuation. This can be due to the high atomic number of Pb compared to the other studied concretes. In other words, higher effective atomic number overcomes higher density in the 18 MeV photon beam. This can be attributed to the predominance of pair production effect in 18 relative to 6 MeV spectrum.

Our results cannot be compared with those of other studies, as this is the first attempt to study attenuation coefficient and TVL for high-density concretes and the wide range of energies used in radiation therapy.

5. Conclusion

As mentioned earlier, there was a lack of attenuation properties for newly proposed heavy concretes in the literature. There was also no comprehensive study on the dosimetric properties of heavy concretes. Using MCNPX MC code, the linear attenuation coefficients of the newly developed high-density concretes were calculated at the photon energy spectra of 4, 6, 10, 15, and 18 MeV Varian linac and ^{60}Co with 1.25 MeV.

Our results showed that with raising the concrete density, linear attenuation coefficient increases, while TVL decreases. Moreover, it was found that for the studied concretes, variation of attenuation coefficient with density was not completely linear. It was concluded that attenuation of high-energy photons in concretes as mixtures not only depends on density of concrete as a material shield, but also on the atomic number of its composing elements.

The data presented in this article can provide new comparative information on the proposed heavy concretes for shielding designers. In addition, based on our calculated data on the studied heavy concretes, medical physics community can have inclusive physical data for designing radiation therapy bunkers.

Acknowledgements

This study was conducted as a part of an MSc thesis in School of Medicine and was financially supported by Immunology Research Center, Faculty of Medicine, Tabriz University of Medical Sciences, Tabriz, Iran.

References

1. Lee SY, Daugherty AM, Broton DJ. Assessing aggregates for radiation-shielding concrete. Concrete international. 2013; 35(5): 31-8.
2. Mesbahi A, Azarpeyvand AA, Shirazi A. Photoneutron production and backscattering in high density concretes used for radiation therapy shielding. Annals of Nuclear Energy. 2011; 38(12): 2752-6.
3. Mesbahi A, Alizadeh G, Seyed-Oskoee G, Azarpeyvand AA. A new barite–colemanite concrete with lower neutron production in radiation therapy bunkers. Annals of Nuclear Energy. 2013; 51: 107-11.
4. Mesbahi A, Azarpeyvand AA, Khosravi HR. Does concrete composition affect photoneutron production inside radiation therapy bunkers?. Japanese journal of radiology. 2012 Feb 1;30(2):162-6.
5. Mesbahi A, Ghiasi H, Mahdavi RS. Photoneutron and capture gamma dose calculations for a radiotherapy room made of high density concrete. Nuclear Technology & Radiation Protection. 2011; 26: 147-52.
6. Ouda A.S. Development of high-performance heavy density concrete using different aggregates for gamma-ray shielding. HBRC Journal. 2014; 11(3): 328-38.
7. Waly ES, Bourham MA. Comparative study of different concrete composition as gamma-ray shielding materials. Annals of Nuclear Energy. 2015; 85: 306-10.

8. Gencel O, Bozkurt A, Kam E, Korkut T. Determination and calculation of gamma and neutron shielding characteristics of concretes containing different hematite proportions. Annals of Nuclear Energy. 2011; 38(12): 2719-23. DOI: 10.1016/j.anucene.2011.08.010.
9. Mortazavi SM, Mosleh-Shirazi MA, Baradaran-Ghahfarokhi M, Siavashpour Z, Farshadi A, Ghafoori M, et al. Production of a datolite-based heavy concrete for shielding nuclear reactors and megavoltage radiotherapy rooms. Iran. J. Radiat. Res. 2010; 8(1): 11-5.
10. Mortazavi SM, Mosleh-Shirazi MA, Roshan-Shomal P, Raadpey N, Baradaran-Ghahfarokhi M. High-performance heavy concrete as a multi-purpose shield. Radiation protection dosimetry. 2010; 142: ncq265.
11. Mortazavi SM, Mosleh-Shirazi MA, Maheri MR, Yousefnia H, Zolghadri S, Haji-pour A. Production of an economic high-density concrete for shielding megavoltage radiotherapy rooms and nuclear reactors. Iran. J. Radiat. Res. 2007; 5(3): 143-6.
12. Aghamiri SM, Mortazavi SM, Shirazi MM, Baradaran-Ghahfarokhi M, Rahmani F, Amiri A, et al. Production of a novel high strength heavy concrete using tourmaline and galena for neutron and photon radiation shielding. Int. J. Radiat. Res. 2014; 12(3): 277-82.
13. Abdo A.E.-S. Calculation of the cross-sections for fast neutrons and gamma-rays in concrete shields. Annals of Nuclear Energy. 2002; 29(16): 1977-88. DOI: 10.1016/S0306-4549(02)00019-1.
14. Sharifi S, Bagheri R, Shirmardi SP. Comparison of shielding properties for ordinary, barite, serpentine and steel–magnetite concretes using MCNP-4C code and available experimental results. Annals of Nuclear Energy. 2013; 53: 529-34. 10.1016/j.anucene.2012.09.015.
15. Shirmardi SP, Shamsaei M, Naserpour M. Comparison of photon attenuation coefficients of various barite concretes and lead by MCNP code, XCOM and experimental data. Annals of Nuclear Energy. 2013; 55: 288-91. DOI: 10.1016/j.anucene.2013.01.002.
16. Oto B, Gür A, Kaçal MR, Doğan B, Arasoğlu A. Photon attenuation properties of some concretes containing barite and colemanite in different rates. Annals of Nuclear Energy. 2013; 51: 120-4. DOI: 10.1016/j.anucene.2012.06.033.
17. Mostofinejad D, Reisi M, Shirani A. Mix design effective parameters on γ-ray attenuation coefficient and strength of normal and heavyweight concrete. Construction and Building Materials. 2012; 28(1): 224-9. DOI: 10.1016/j.conbuildmat.2011.08.043.
18. Stanković SJ, Ilić RD, Janković K, Bojović D, Lončar B. Gamma radiation absorption characteristics of concrete with components of different type materials. Acta Physica Polonica A. 2010; 117(5): 812-6.
19. Akkurt I, Akyildirim H, Mavi B, Kilincarslan S, Basyigit C. Gamma-ray shielding properties of concrete including barite at different energies. Progress in Nuclear Energy. 2010; 52(7): 620-3. DOI: 10.1063/1.4976488.
20. Demir F, Budak G, Sahin R, Karabulut A, Oltulu M, Şerifoğlu K, et al. Radiation transmission of heavyweight and normal-weight concretes containing colemanite for 6MV and 18MV X-rays using linear accelerator. Annals of Nuclear Energy. 2010; 37(3): 339-44. DOI: 10.1016/j.anucene.2009.12.010.
21. Akkurt I, Kilincarslan S, Basyigit C. The photon attenuation coefficients of barite, marble and limra. Annals of Nuclear Energy. 2004; 31(5): 577-82. DOI: 10.1016/j.anucene.2003.07.002.
22. Akkurt I, Basyigit C, Kilincarslan S, Mavi B, Akkurt A. Radiation shielding of concretes containing different aggregates. Cement and Concrete Composites. 2006; 28(2): 153-7. DOI: 10.1016/j.cemconcomp.2005.09.006.
23. Bouzarjomehri F, Bayat T, Dashti MH, Ghisari J, Abdoli N. 60 Co γ-ray attenuation coefficient of barite concrete. Iranian Journal of Radition Research(Print). 2006; 4: 71-5.
24. Demir F, Budak G, Sahin R, Karabulut A, Oltulu M, Un A. Determination of radiation attenuation coefficients of heavyweight-and normal-weight concretes containing colemanite and barite for 0.663 MeV γ-rays. Annals of Nuclear Energy. 2011; 38(6): 1274-8. DOI: 10.1016/j.anucene.2011.02.009.
25. Abdo AE, Kansouh WA, Megahid RM. Investigation of radiation attenuation properties for baryte concrete. Japanese journal of applied physics. 2002; 41(12R): 7512. DOI: 10.1143/JJAP.41.7512.
26. Picha R, Channuie J, Khaweerat S, Liamsuwan T, Promping J, Ratanatongchai W, et al. Gamma and neutron attenuation properties of barite-cement mixture. Paper presented at the Journal of Physics: Conference Series; 2015.
27. Calzada E, Grünauer F, Schillinger B, Türck H. Reusable shielding material for neutron-and gamma-radiation. Nuclear Instruments and Methods in Physics Research Section A: Accelerators, Spectrometers, Detectors and Associated Equipment. 2011; 651(1): 77-80. DOI: 10.1016/j.nima.2010.12.239.
28. Singh VP, Ali AM, Badiger NM, El-Khayatt AM. Monte Carlo simulation of gamma ray shielding parameters of concretes. Nuclear Engineering and Design. 2013; 265: 1071-7. DOI: 10.1016/j.nucengdes.2013.10.008.
29. Facure A, Silva AX. The use of high-density concretes in radiotherapy treatment room design. Applied Radiation and Isotopes. 2007; 65(9): 1023-8. DOI: 10.1016/j.apradiso.2007.04.006.
30. Bashter I. Calculation of radiation attenuation coefficients for shielding concretes. Annals of nuclear Energy. 1997; 24(17): 1389-401.

31. Bashter II, Abdo AE, Abdel-Azim MS. Magnetite ores with steel or basalt for concrete radiation shielding. Japanese journal of applied physics. 1997; 36(6R): 3692-6. DOI: 10.1143/JJAP.36.3692.
32. NCRP. National council on radiation protection and measurements, NCRP No. 144. Radiation protection for particle accelerator facilities. 2003; 1-499.
33. NCRP. National Council on Radiation Protection and Measurements, NCRP No. 151. Structural Shielding Design and Evaluation for Megavoltage X- and Gamma-Ray Radiotherapy Facilities. Annals of Nuclear Energy. 2005; 1-246.
34. Sheikh-Bagheri D, Rogers DW. Monte Carlo calculation of nine megavoltage photon beam spectra using the BEAM code. Medical physics. 2002; 29(3): 391-402. DOI: 10.1118/1.1445413.
35. Pelowitz DB, Durkee JW, Elson JS, Fensin ML, Hendricks JS, James MR, et al. MCNPX 2.7 E extensions. Los Alamos National Laboratory (LANL); 2011 Mar 7.
36. Attix F.H. Introduction to radiological physics and radiation dosimetry. John Wiley & Sons; 2008.
37. Hendee W.R. and E.R. Ritenour. Medical imaging physics. John Wiley & Sons; 2003.
38. Martin J.E. Physics for radiation protection: a handbook. John Wiley & Sons; 2006.
39. Chang DS, Lasley FD, Das IJ, Mendonca MS, Dynlacht JR. Basic radiotherapy physics and biology. Springer; 2014 Sep 19.
40. Dowsett D, Kenny PA, Johnston RE. The Physics of Diagnostic Imaging Second Edition. CRC Press; 2006 Apr 28.
41. Ekolu, S, M.A. Ramushu. Radiological assessment of high density shielding concrete for neutron radiography. Paper presented at the Intl Conf. on Construction Materials and Structures; 2014.
42. Lorente, A, E. Gallego, H.R. Vega-Carrillo, R. Méndez. Neutron shielding properties of a new high-density concrete. Paper presented at the 12th International Congress of the International Radiation Protection Association, IRPA-12, Buenos Aires, Argentina; 2008.
43. Makarious AS, Bashter II, Abdo AE, Azim MS, Kansouh WA. On the utilization of heavy concrete for radiation shielding. Annals of Nuclear Energy. 1996; 23(3): 195-206. DOI: 10.1016/0306-4549(95)00021-1.
44. Akkurt I, Basyigit C, Kilincarslan S, Mavi B. The shielding of γ-rays by concretes produced with barite. Progress in Nuclear Energy. 2005; 46(1): 1-11. DOI: 10.1016/j.pnucene.2004.09.015.
45. Wang J, Li G, Meng D. Evaluation of the performance of peridotite aggregates for radiation shielding concrete. Annals of Nuclear Energy. 2014; 71: 436-9. DOI: 10.1016/j.anucene.2014.04.012.
46. Akkurt I, Mavi B, Akkurt A, Basyigit C, Kilincarslan S, Yalim HA. Study on Z dependence of partial and total mass attenuation coefficients. Journal of Quantitative Spectroscopy and Radiative Transfer. 2005; 94(3): 379-85. DOI: 10.1016/j.jqsrt.2004.09.024.
47. Cember H, T Johnson. Introduction to Health Physics: Fourth Edition (Fourth ed.): McGraw Hill Professional; 2008.
48. Hubbell JH, Seltzer SM. Tables of x-ray mass attenuation coefficients and mass energy-absorption coefficients 1 keV to 20 MeV for elements Z= 1 to 92 and 48 additional substances of dosimetric interest. National Inst. of Standards and Technology-PL, Gaithersburg, MD (United States). Ionizing Radiation Div.; 1995 May 1.
49. Gerward L, Guilbert N, Jensen KB, Levring H. WinXCom—a program for calculating X-ray attenuation coefficients. Radiation physics and chemistry. 2004; 71(3): 653-4. DOI: 10.1016/j.radphyschem.2004.04.040.
50. Wood J. Computational methods in reactor shielding: Elsevier; 2013.